PROCEEDINGS OF SPIE

SPIEDigitalLibrary.org/conference-proceedings-of-spie

Hybrid microscopy of human carotid atheroma by means of optical-resolution optoacoustic and non-linear optical microscopy

Markus Seeger, Angelos Karlas, Dominik Soliman, Jaroslav Pelisek, Vasilis Ntziachristos

Markus Seeger, Angelos Karlas, Dominik Soliman, Jaroslav Pelisek, Vasilis Ntziachristos, "Hybrid microscopy of human carotid atheroma by means of optical-resolution optoacoustic and non-linear optical microscopy," Proc. SPIE 10064, Photons Plus Ultrasound: Imaging and Sensing 2017, 1006455 (3 March 2017); doi: 10.1117/12.2254891



Event: SPIE BiOS, 2017, San Francisco, California, United States

Hybrid microscopy of human carotid atheroma by means of opticalresolution optoacoustic and non-linear optical microscopy

Markus Seeger^{a,b}, Angelos Karlas^{a,b,c}, Dominik Soliman^{a,b}, Jaroslav Pelisek^d, Vasilis Ntziachristos^{a,b*}

^aChair for Biological Imaging, Technische Universität München, Munich, Germany

^dDepartment of Vascular and Endovascular Surgery, Klinikum rechts der Isar, Technische Universität München, Munich, Germany

*Correspondence to v.ntziachristos@tum.de

ABSTRACT

Carotid atheromatosis is causally related to stroke, a leading cause of disability and death. We present the analysis of a human carotid atheroma using a novel hybrid microscopy system that combines optical-resolution optoacoustic (photoacoustic) microscopy and several non-linear optical microscopy modalities (second and third harmonic generation, as well as, two-photon excitation fluorescence) to achieve a multimodal examination of the extracted tissue within the same imaging framework. Our system enables the label-free investigation of atheromatous human carotid tissue with a resolution of about 1 μ m and allows for the congruent interrogation of plaque morphology and clinically relevant constituents such as red blood cells, collagen, and elastin. Our data reveal mutual interactions between blood embeddings and connective tissue within the atheroma, offering comprehensive insights into its stage of evolution and severity, and potentially facilitating the further development of diagnostic tools, as well as treatment strategies.

Keywords: Human carotid atheroma, Collagen, Red blood cells, Multimodal microscopy, Optoacoustic microscopy, Photoacoustic microscopy, Non-linear optical microscopy

1. INTRODUCTION

Stroke is one of the major causes of morbidity and mortality in the western world. Carotid artery atherosclerosis and its complications is the main culprit of stroke, rendering the intensive investigation of atheroma pathology and pathophysiology a critical need¹. Ischemic stroke secondary to carotid atherosclerosis is a frequent medical emergency that needs urgent treatment. In this respect, an atheromatous plaque, which progressively accumulates within the subendothelial layer (intima) of the affected artery, becomes complicated and causes an acute thrombotic luminal occlusion and cerebral ischemia. On the quest for a reliable method to early detect lesions strongly precipitating to acute ischemic events, identifying the mechanisms underlying plaque formation and rupture is of critical need.

Over the last decades, many theories have been developed regarding the pathogenesis of atherosclerosis and numerous studies explored the role of several biological constituents such as lipids, inflammatory and smooth muscle cells (SMC), connective tissue, and calcium deposits²⁻⁴. Multiple factors (e.g. inflammatory, biomechanical, genetic, environmental) seem to get involved in all stages of atheroma formation and progression⁴. Each lesion follows several evolutionary stages corresponding to subsequent steps of the atherosclerotic process and different pathological profiles. Although lesions could remain clinically silent over decades, a stable plaque may become vulnerable, get destabilized, and finally complicated (ulcerated, fissured, ruptured) leading to ischemic symptoms and tissue necrosis³.

Along their evolutionary progress, atheromas can be assigned to different classes according to their degree of severity: early, intermediate, and advanced stage⁵. Asymptomatic lesions (early) are characterized by macrophage clusters (Type I) followed by the formation of patches containing layered foam cells and lipid-loaded SMCs (Type II)⁶. Type I and II lesions are characterized by the early presence of intimal thickening and xanthoma without demonstrating any

Photons Plus Ultrasound: Imaging and Sensing 2017, edited by Alexander A. Oraevsky, Lihong V. Wang, Proc. of SPIE Vol. 10064, 1006455 ⋅ © 2017 SPIE ⋅ CCC code: 1605-7422/17/\$18 ⋅ doi: 10.1117/12.2254891

^bInstitute of Biological and Medical Imaging, Helmholtz Zentrum München, Neuherberg, Germany

^cDepartment of Cardiology, Klinikum rechts der Isar, Technische Universität München, Munich, Germany

pathological changes over time⁵. Furthermore, a transitional early plaque type (Type III) shows a pattern of lipidic regions distributed among the layers of SMCs and a pathologic intimal thickening⁶. These are the first lesions that may progress to an acute thrombotic complication and a clinical event via plaque ulceration⁵. Starting from intermediate lesions of Type IV, plaques are called atheromas and are characterized by a distinct lipid core covered by a fibrous cap. Atheromas usually protrude into the vascular lumen and their cap may get fissured or ulcerated and, thus, lead to a thrombus formation^{5,6}. However, the risk of plaque rupture and acute events depends mainly on plaque composition and not on plaque size or luminal constriction^{7,8}. The most dangerous lesions (Type V and VI) are classified as advanced (late) and complicated plaques. Whereas Type V lesions develop a thin fibrous cap and a large lipid core, and contain more collagen and SMCs, Type VI lesions are further complicated by superficial fissure formation, intraplaque hemorrhage (IPH), and acute luminal thrombus occurrence^{4,5,9}. In terms of clinical phenotype, early lesions are asymptomatic while intermediate ones may cause ischemic disturbances^{7,9}. Finally, rupture of an advanced plaque may be followed by local healing or thrombus formation with or without complete vascular occlusion.

The general topography of plaques can be partitioned into discrete areas such as the cap, the shoulders, and the lipid core (see *Fig. 2a*). Thrombosis is usually actuated by a plaque rupture in the shoulder region combined with an ulceration of the cap²⁻⁴. A large necrotic core consisting of lipids, blood cells, macrophages and fibrin, a thinned cap of degraded collaged and SMCs, as well as the presence of inflammation and neovascularization indicate the vulnerability of the plaque¹⁰. Moreover, mechanical injury is commonly assumed to be an important underlying mechanism of rupture. Hence, observing and analyzing components, such as collagen and elastin, fundamental parts of the connective tissue regulating the mechanical stability of an atherosclerotic lesion, is of great interest¹¹. Furthermore, intraplaque blood in form of neovessels or IPH seem to contribute significantly to the progression and rupture of the plaque¹⁰.

Histopathological interrogation of atheromas is primarily based on staining methods, which enables the microscopic depiction of several cellular and molecular features ^{12–16}. In this case, multiple adjacent slices are required to visualize the components of interest, not only making this procedure costly and ineffective, but also preventing an accurate superimposition of the observed components. Thus, a variety of approaches have been introduced to examine human carotid atheroma using label-free multimodal imaging techniques which visualize intrinsic contrast by nonlinear optical (NLO) phenomena^{17–22}. Since NLO processes rely on specific optical properties of the imaged tissue for harmonic generation or high quantum yield based autofluorescence generated by multiphoton absorption²³, these methods are not or only partially able to detect blood residues within the plaque in a label-free mode. In order to image coagulated blood within the scope of inflammation, neovascularisation, and IPH, standard histology methods such as immunochemistry and simple staining are commonly employed¹².

Developing or utilizing imaging systems, which are able to depict the above mentioned constituents involved in the plaque formation and destabilization and their mutual interactions at a very high resolution (1 μ m), could enable new insights into the process of atherosclerosis. Therefore, we developed a novel method of characterizing atheromatous tissue using a hybrid multiphoton and optoacoustic microscopy system (MPOM). The setup allows for co-registered visualization of several components of interest in one atheromatous slice without the need of chemical staining of different slices. In this study, we focus mainly on collagen and red blood cell (RBC) visualization, two basic components which are present and frequently altered in unstable plaques¹².

2. MATERIAL AND METHODS

2.1 Experimental setup

The hybrid multiphoton and optoacoustic microscopy (MPOM) system of this study (see *Fig. 1*), as comprehensively described and characterized in^{24–26}, relies on the combination of laser-scanning modalities such as second and third harmonic generation (SHG and THG), two-photon excitation fluorescence (TPEF), and optical-resolution optoacoustic microscopy (OR-OAM). MPOM utilizes two separate excitation sources for the non-linear optical (NLO) signals and the optoacoustic effect, which are co-aligned and commonly guided over a set of galvanometric mirrors (GM) (6215H, Cambridge Technology, Bedford, USA) in order to raster-scan both foci across the specimen placed onto an inverted microscope (AxioObserver.D1, Zeiss, Jena, Germany). Finally, a lateral resolution of about 1 μm across a field of view (FOV) of about 630 x 630 μm² is achieved for all modalities by using a microscope objective lens (Plan Apochromat 10X, Zeiss, Jena, Germany; air immersion, NA: 0.45)^{24–26}. The system is fully controlled in Matlab (Matlab 2014a, Mathworks, Natick, USA). All MPOM images shown in this work are acquired with a resolution of 600 x 600 pixels and an averaging of 50. For validation purposes, MPOM also equips a CCD camera (AxioCam ICc 1, Zeiss) to take

microscopic brightfield (BF) images of the specimen, whereas widefield BF examinations are carried out on a separate microscope (Aperia CS2, Leica, Wetzlar, Germany).

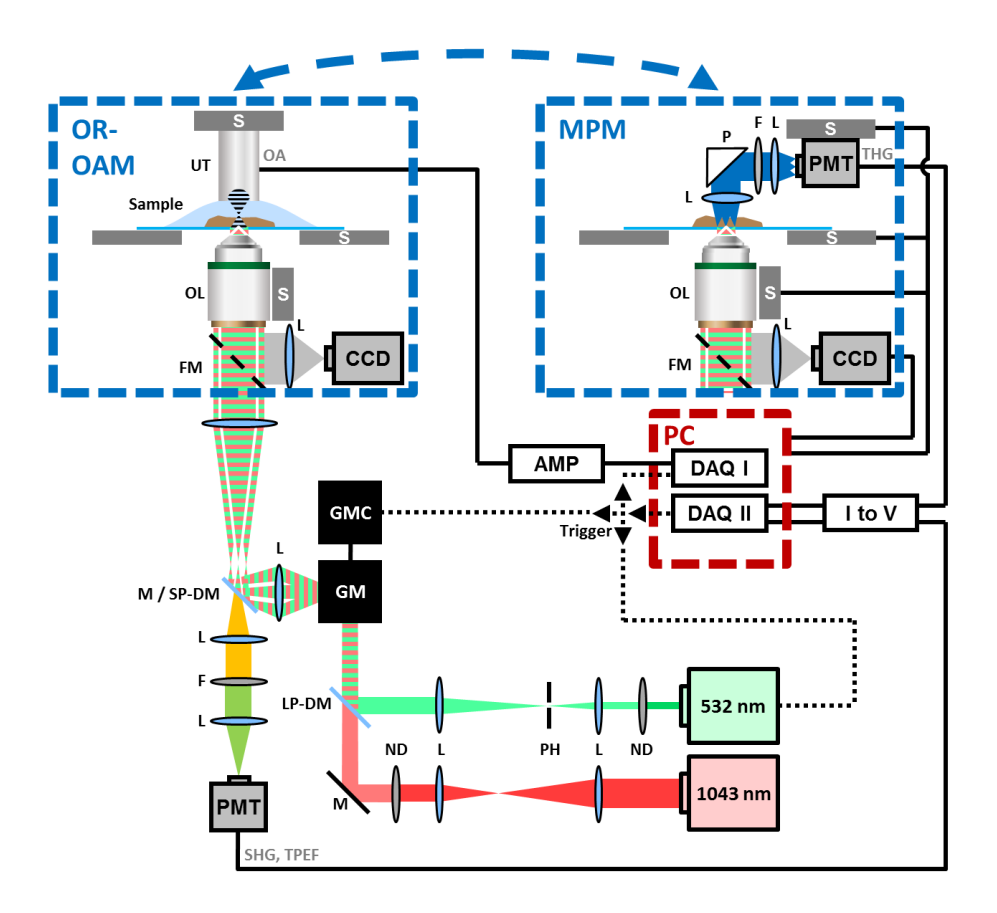


Figure 1. Schematic depiction of MPOM consisting of two interchangeable microscopy systems, namely OR-OAM and MPM. Abbreviations: AMP, amplifier; DAQ, data acquisition card; F, optical filter; FM, flippable mirror; GM, galvanometric mirrors; GMC, GM control; L, lens; LP-DM, longpass dichroic mirror; M, mirror; ND, neutral density filter; OA, optoacoustic signal; OL, microscope objective lens; P, prism; PH, pinhole; PMT, photomultiplier tube; S, xyz stage; SHG, second harmonic generation signal; SP-DM, shortpass dichroic mirror; UT, ultrasound transducer; THG, third harmonic generation signal; TPEF, two-photon excitation fluorescence signal.

Optoacoustic microscopy (OAM). The optoacoustic modality equips an actively Q-switched diode-pumped solid-state laser (SPOT-10-200-532, Elforlight, Daventry, UK; energy per pulse: 20 μJ, pulse width: 1.8 ns, repetition rate: 50 kHz) as an excitation source at 532 nm. The beam is spatially filtered by a pinhole, attenuated by a set of neutral density filters, merged with the other laser beam by a longpass dichroic mirror (DMLP650, Thorlabs, New Jersey, USA), guided onto a high-precision set of GMs, and finally focused into the specimen as described previously. In order to achieve high-speed OAM acquisition, the laser, the GMs, as well as the acquisition of the OAM signals detected by a spherically focused 100 MHz transducer (SONAXIS, Besancon, France; bandwidth: ~10-180 MHz, focal distance: 2.85 mm, active element diameter: 3 mm) placed in positive defocus and amplified by 63 dB (AU 1291, Miteq, New York, USA) are actively triggered by a 16 bit data acquisition card (DAQ) (PCIe 6363, National Instruments, Austin, Texas, USA; max. sampling rate per channel: 1 MS/s). The raw OAM signals are recorded by a high-speed 12 bit DAQ card (ADQ412, SP Devices, Linköping, Sweden; max. sampling rate per channel: 4 GS/s) in a streaming-like acquisition mode at 900 MS/s ²⁶. Due to the active triggering of all involved components, a direct assignment of the recorded OAM signals to the corresponding pixel in the final image is enabled. The signals are further bandpass filtered from 10 to 180 MHz and their maximum amplitude projection (MAP) is used for final image generation.

Multiphoton microscopy (MPM). As described comprehensively in^{24–26}, a Yb-based solid-state laser (YBIX, Time-Bandwidth, Zurich, Switzerland; energy per pulse: 30 nJ, pulse width: 170 fs, repetition rate: 84.4 MHz) is utilized to generate NLO signals such as SHG, THG, and TPEF. Using optical filters (SHG (FB520-10), THG (FGUV11), TPEF (FELH0550), Thorlabs) and highly sensitive PMTs (H9305-03, Hamamatsu, Hamamatsu City, Japan), these signals are digitized by the previously mentioned 16 bit DAQ card, which also controls the GM scanning with a predefined scanning frequency of 320 kHz.

2.2 Imaging protocol

The human atherosclerotic tissue sample was extracted by carotid thrombendarterectomy (CAE) from a patient with advanced carotid artery stenosis. The plaque was first cut into blocks of about 3 mm length, fixed in formalin, embedded in paraffin, and cut into 20 µm thick slices, that were finally placed onto glass slides (170 µm)²⁶. In order to select ROIs for latter high-resolution MPOM examination, the yellow-brownish pattern seen in a widefield BF image of the whole specimen (Aperio CS2, Leica) is assigned to a coarse mechanical OAM scan over an 8 x 8 mm² FOV utilizing the sample holding xyz-stage (MLS203-2 & MZS500, Thorlabs). Image processing and co-registration of all MPOM modalities was carried out in ImageJ (ImageJ 1.51g, Wayne Rasband) as described in²⁶.

3. RESULTS

Prior to MPOM investigation of the atherosclerotic tissue sample, we imaged the whole specimen with both a widefield BF and coarse OAM scan which was further assigned to typical topological regions within the plaque (see *1. Introduction*) as depicted in Fig. 2a. Fig. 2b shows a widefield BF image of the sample. In Fig. 2c, a coarse OAM scan of the whole sample can be seen, which is co-registered to the widefield BF image according to the yellow-brown pattern across the sample that is assumed as intraplaque blood embeddings.

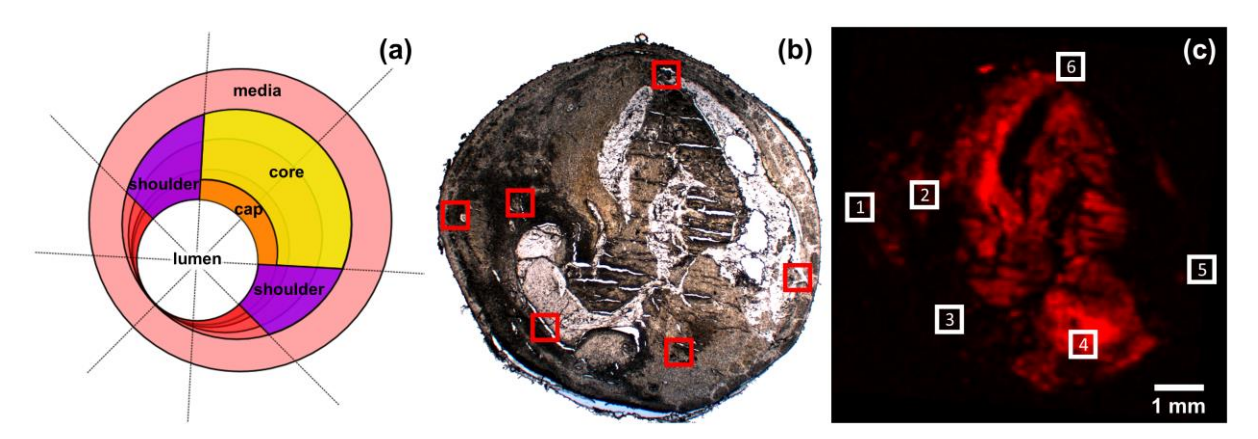


Figure 2. Coarse examination and ROI selection of human carotid atheroma. (a) Schematic subdivision of an atheroma tissue slice. (b) Widefield BF image of the unstained atheroma sample and (c) coarse OAM scan reveal an advanced stage characterized by large tissue fissures and significant intraplaque RBC embedding. Final ROI selection for subsequent MPOM imaging is indicated by the red or white boxes.

As becomes apparent in Fig. 2, the atherosclerotic tissue sample is characterized by large fissures, a highly degraded tissue morphology and a widely spread blood embedding. Thus, an advanced stage of the lesion (Type VI) could be assumed. To further study the fine topological features of the sample we chose 6 ROIs across the specimen to perform high-resolution MPOM examination.

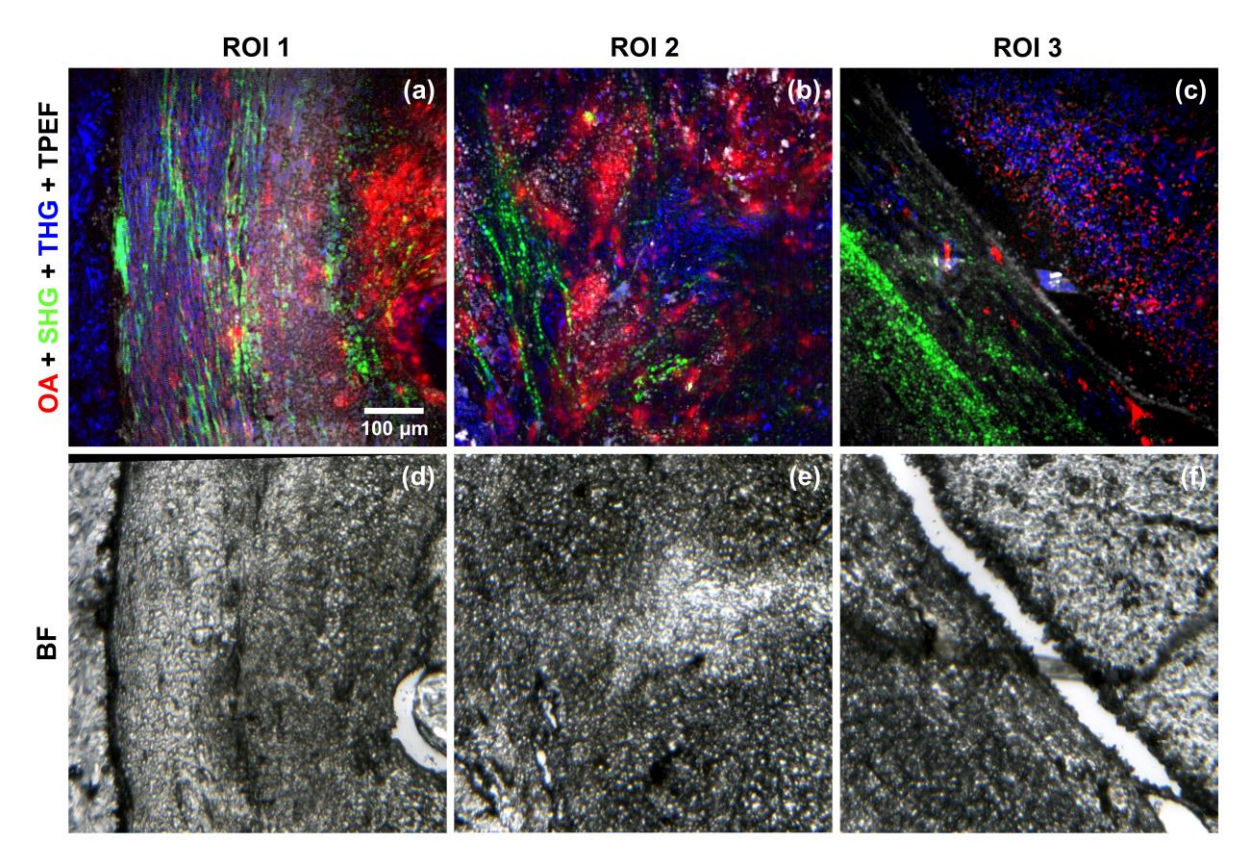


Figure 3. Hybrid microscopy imaging of human carotid atheroma at the shoulder and cap region. (a) Overlay of OA, SHG, THG, and TPEF demonstrates a largely unscathed condition of the connective tissue (e.g. collagen and elastin), no large inclusions or fissures, and blood residues at the side in ROI 1. Analogous depiction of **(b)** ROI 2 reveals partly intact connective tissue and widely spread blood embeddings and of **(c)** ROI 3 two separated areas of connective tissue and inclusions of single erythrocytes. **(d-f)** Corresponding BF observation of (a-c), respectively.

Fig. 3 depicts the MPOM examination of ROI 1, ROI 2, and ROI 3, which are located close to the former lumen in the shoulder and the cap region (see *Fig.* 2). Fig. 3a presents a composite image combining OAM, SHG, THG, and TPEF images of ROI 1. Here, a largely maintained connective tissue of collagen and elastin can be seen, whereas the collagen and elastin fibrils appear spread into single fibers. A spatially separated blood inclusion is located towards to former lumen. Fig. 3b shows an analogous examination of ROI 2 revealing a partly intact collagen fibril band of roughly 100 μm width consisting of individual strands and a widely spread blood embedding. In Fig. 3c, two separated areas can be observed. Herein, one side contains collagen and elastin as part of the connective tissue whereas the other side is characterized by areas of diffuse single erythrocytes. The corresponding BF images shown in Fig. 3d-f demonstrate, besides the large rupture in ROI 3 separating the two mentioned regions, the overall unharmed tissue morphology in these ROIs.

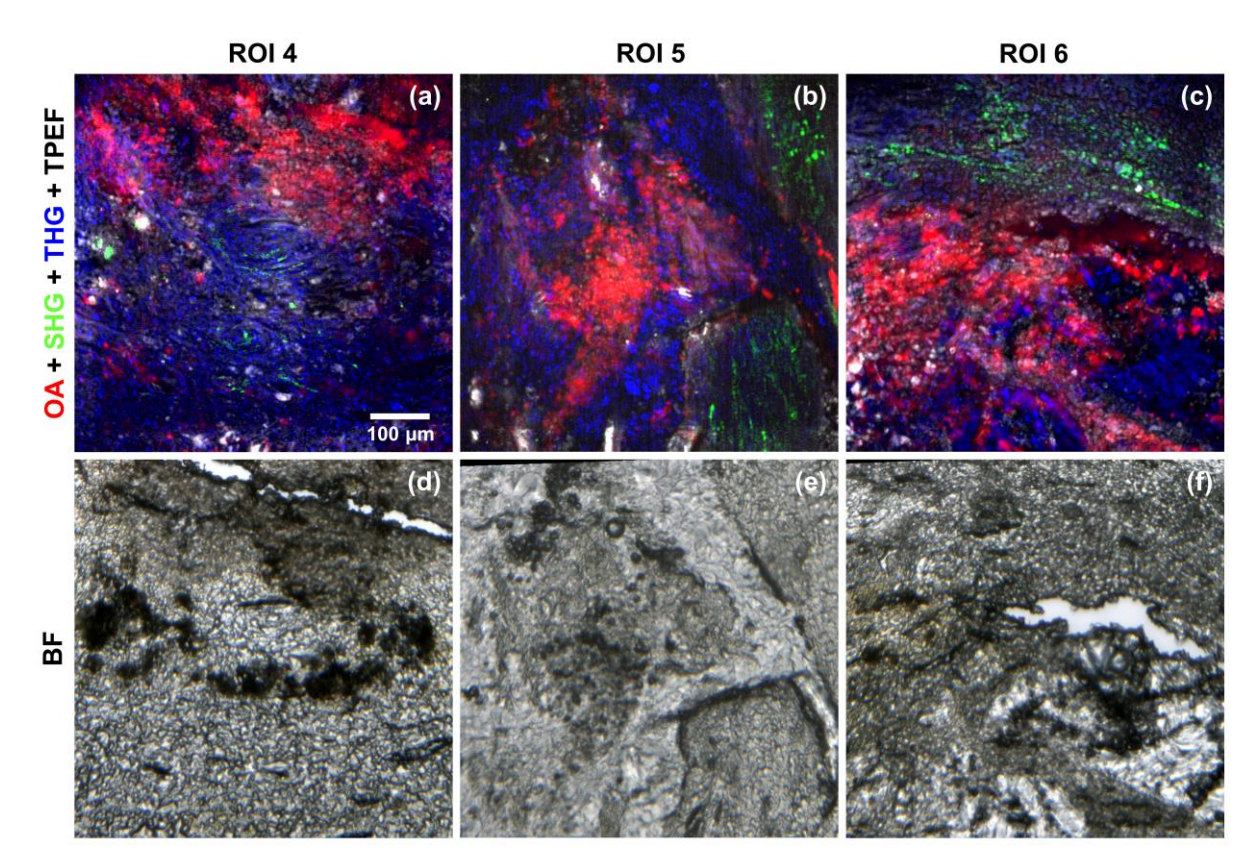


Figure 4. Hybrid microscopy imaging of human carotid atheroma in the lipid core. (a) Overlay of OA, SHG, THG, and TPEF indicates a highly degraded connective tissue (e.g. collagen and elastin), inclusions and fissures, and blood embeddings at the top part in ROI 4. Analogous depiction of (b) ROI 5 demonstrates residues of connective tissue and spatially separated blood inclusions along with a highly distorted tissue morphology. In ROI 6 (c), two separated areas of intact connective tissue and blood residues can be seen together with a highly damaged morphology. (d-f) Corresponding BF observation of (a-c), respectively.

Fig. 4 shows MPOM images from ROI 4-6 located at the lipid core close to the media layer of the plaque (see *Fig.* 2). As before, the merged image is shown in Fig. 4a-c and the corresponding BF images are shown in Fig. 4d-f, respectively. Fig. 4a depicts a highly degraded connective tissue without the presence of intact collagen and elastin bands. Furthermore, blood embeddings can be seen at the top part in this ROI. In Fig. 4b and c, showing the ROIs 5 and 6 located close to the media layer of the plaque, partly intact connective tissue is observable indicating the boundary to the media layer. Furthermore, a widely spread blood residue pattern can be seen. In these two ROIs, the tissue morphology revealed by THG and BF is characterized by large fissures and ruptures in the range of 50-100 μm.

4. DISCUSSION

In this work, we imaged and characterized a human carotid atheroma sample using a novel-developed a label-free hybrid microscope by means of optical resolution optoacoustic microscopy along with non-linear optical microscopy. Hybrid microscopy utilizing contrast mechanisms without the need of staining and labelling offers the unique possibility to depict several moieties of interest within the same slice of the sample. Due to this property, a co-registered depiction with a sub-micrometer precision and resolution of relevant atheroma elements such as blood embeddings, the connective tissue consisting of collagen and elastin, as well as the overall tissue morphology is enabled. Hence, mutual interactions can be investigated leading to new insights into pathological phenomena.

We studied a human carotid atheroma sample of a patient with severe and advanced stage of atherosclerosis. The developed hybrid multiphoton and optoacoustic microscopy (MPOM) revealed several structural and morphological features within the sample. By using OAM, hemoglobin, a natural strong near-infrared light absorber, can be detected

and visualized. Collagen and elastin, as parts of the connective tissue, can be imaged by SHG and TPEF, respectively, whereas the tissue morphology is revealed by THG and BF observations. These components play a crucial role in the viscoelastic behavior, stability, and stress tolerance of the vessel wall^{26,27}. In a healthy arterial wall, intact connective tissue adapts to wall stresses, and enhances the mechanical strength. During the progress of atherosclerotic disease, both overproduction of connective tissue, which leads to stenosis, as well as, its degradation are assumed to influence the plaque vulnerability²⁸. Besides that, embeddings of RBCs in the form of neovascularisation and IPH are considered to contribute to the accumulation of atheromatous mass^{29,30}. Revealed by standard histological studies, a plaque at risk of rupture is characterized by a large lipid core, degraded connective tissue within the fibrous cap, severe inflammation in the shoulder regions and the cap, and significant accumulation of blood embeddings^{16,26}.

In this study, MPOM examined these biological features without the need of staining and, thus, enabled the precise depiction of co-registered distributions and their mutual interactions. Our results indicate several different conditions ranging from intact connective tissue as part of the media layer along with embeddings of diffuse single RBCs and minor blood clusters to a highly degraded connective tissue with a widely spread blood inclusion. With the background knowledge of a severe state of the extracted plaque together with the previously demonstrated examination of an advanced atheroma²⁶, these findings confirm a mutual interaction among intraplaque blood embeddings and the connective tissue on the single cell or strand level. Future investigations of human carotid atheromas in different pathological stages of the disease could offer new insights in the overall process of the accumulation of atheroma, the degradation of the connective tissue, the occurrences of intraplaque blood residues, and, finally, caused effects on the plaques vulnerability. Furthermore, along with macroscopic *in vivo* observations by means of multispectral optoacoustic tomography (MSOT)³¹, an improved diagnostic method as well as novel treatment strategies could be investigated.

ACKNOWLEDGEMENTS

The authors acknowledge funding from the DFG as part of the CRC 1123 (Z1) and the DFG Reinhard Koselleck project (NT 3/9-1).

REFERENCES

- [1] WHO, 2014, "WHO | The top 10 causes of death," in Fact sheet N°310 (Updated May 2014), World Health Organization (2014).
- [2] Insull, W., "The Pathology of Atherosclerosis: Plaque Development and Plaque Responses to Medical Treatment," American Journal of Medicine 122(1 SUPPL.), S3–S14 (2009).
- [3] Dickson, B.C., and Gotlieb, A.I., "Towards understanding acute destabilization of vulnerable atherosclerotic plaques," Cardiovascular Pathology 12(5), 237–248 (2003).
- [4] Singh, R.B., Mengi, S.A., Xu, Y.J., Arneja, A.S., and Dhalla, N.S., "Pathogenesis of atherosclerosis: A multifactorial process," in Exp. Clin. Cardiol. 7(1), pp. 40–53 (2002).
- Virmani, R., Burke, A., Ladich, E., and Kolodgie, F.D., "Pathology of carotid artery atherosclerotic disease," Carotid Disease. 1st ed. Cambridge University Press, Cambridge, United Kingdom1–2 (2007).
- [6] Stary, H.C., Chandler, A.B., Glagov, S., Guyton, J.R., Insull Jr., W., Rosenfeld, M.E., Schaffer, S.A., Schwartz, C.J., Wagner, W.D., et al., "A definition of initial, fatty streak, and intermediate lesions of atherosclerosis. A report from the Committee on Vascular Lesions of the Council on Arteriosclerosis, American Heart Association," Circulation 89(5), 2462–2478 (1994).
- [7] Gutstein, D.E., and Fuster, V., "Pathophysiology and clinical significance of atherosclerotic plaque rupture," in Cardiovasc. Res. 41(2), pp. 323–333 (1999).
- [8] Mann, J.M., and Davies, M.J., "Vulnerable plaque. Relation of characteristics to degree of stenosis in human coronary arteries.," Circulation 94(5), 928–31 (1996).
- [9] Stary, H.C., Chandler, A.B., Dinsmore, R.E., Fuster, V., Glagov, S., Insull, W., Rosenfeld, M.E., Schwartz, C.J., Wagner, W.D., et al., "A Definition of Advanced Types of Atherosclerotic Lesions and a Histological Classification of Atherosclerosis: A Report From the Committee on Vascular Lesions of the Council on Arteriosclerosis, American Heart Association," Circulation 92(5), 1355–1374 (1995).
- [10] Chistiakov, D.A., Orekhov, A.N., and Bobryshev, Y. V, "Contribution of neovascularization and intraplaque haemorrhage to atherosclerotic plaque progression and instability," in Acta Physiol. 213(3), pp. 539–553 (2015).

- [11] Nadkarni, S.K., Bouma, B.E., De Boer, J., and Tearney, G.J., "Evaluation of collagen in atherosclerotic plaques: The use of two coherent laser-based imaging methods," in Lasers Med. Sci. 24(3), pp. 439–445 (2009).
- [12] Purushothaman, K.-R., Purushothaman, M., Muntner, P., Lento, P. a, O'Connor, W.N., Sharma, S.K., Fuster, V., and Moreno, P.R., "Inflammation, neovascularization and intra-plaque hemorrhage are associated with increased reparative collagen content: implication for plaque progression in diabetic atherosclerosis.," Vascular medicine (London, England) 16(2), 103–8 (2011).
- [13] Bentzon, J.F., Otsuka, F., Virmani, R., and Falk, E., "Mechanisms of Plaque Formation and Rupture," Circulation Research 114(12), 1852–1866 (2014).
- [14] Virmani, R., "Atherosclerotic Plaque Progression and Vulnerability to Rupture: Angiogenesis as a Source of Intraplaque Hemorrhage," Arteriosclerosis, Thrombosis, and Vascular Biology 25(10), 2054–2061 (2005).
- [15] Milei, J., Parodi, J.C., Ferreira, M., Barrone, A., Grana, D.R., and Matturri, L., "Atherosclerotic plaque rupture and intraplaque hemorrhage do not correlate with symptoms in carotid artery stenosis," Journal of Vascular Surgery 38(6), 1241–1247 (2003).
- [16] Virmani, R., Kolodgie, F.D., Burke, A.P., Farb, A., and Schwartz, S.M., "Lessons From Sudden Coronary Death," Arteriosclerosis & Thrombosis1262–1275 (2000).
- [17] Mostaço-Guidolin, L.B., Sowa, M.G., Ridsdale, A., Pegoraro, A.F., Smith, M.S.D., Hewko, M.D., Kohlenberg, E.K., Schattka, B., Shiomi, M., et al., "Differentiating atherosclerotic plaque burden in arterial tissues using femtosecond CARS-based multimodal nonlinear optical imaging," Biomedical optics express 1(1), 59–73 (2010).
- [18] Le, T.T., Langohr, I.M., Locker, M.J., Sturek, M., and Cheng, J.-X., "Label-free molecular imaging of atherosclerotic lesions using multimodal nonlinear optical microscopy," Biomedical microdevices 12(5), 1–20 (2009).
- [19] Van Zandvoort, M., Engels, W., Douma, K., Beckers, L., Oude Egbrink, M., Daemen, M., and Slaaf, D.W., "Two-Photon Microscopy for Imaging of the (Atherosclerotic) Vascular Wall: A Proof of Concept Study," Journal of Vascular Research 41(1), 54–63 (2004).
- [20] Massberg, S., Brand, K., Gruner, S., Page, S., Muller, E., Muller, I., Bergmeier, W., Richter, T., Lorenz, M., et al., "A critical role of platelet adhesion in the initiation of atherosclerotic lesion formation," J. Exp. Med. 196(7), 887–896 (2002).
- [21] Massberg, S., Gawaz, M., Gruner, S., Schulte, V., Konrad, I., Zohlnhofer, D., Heinzmann, U., and Nieswandt, B., "A Crucial Role of Glycoprotein VI for Platelet Recruitment to the Injured Arterial Wall In Vivo," Journal of Experimental Medicine 197(1), 41–49 (2002).
- Yu, W., Braz, J.C., Dutton, A.M., Prusakov, P., and Rekhter, M., "In vivo imaging of atherosclerotic plaques in apolipoprotein E deficient mice using nonlinear microscopy.," Journal of biomedical optics 12(5), 54008 (2007).
- [23] Chen, X., Nadiarynkh, O., Plotnikov, S., and Campagnola, P.J., "Second harmonic generation microscopy for quantitative analysis of collagen fibrillar structure," Nat Protoc 7(4), 654–669 (2012).
- [24] Soliman, D., Tserevelakis, G.J., Omar, M., and Ntziachristos, V., "Combining microscopy with mesoscopy using optical and optoacoustic label-free modes," Nature Publishing Group1–9 (2015).
- [25] Tserevelakis, G.J., Soliman, D., Omar, M., and Ntziachristos, V., "Hybrid multiphoton and optoacoustic microscope.," Optics letters 39(7), 1819–22 (2014).
- [26] Seeger, M., Karlas, A., Soliman, D., Pelisek, J., and Ntziachristos, V., "Multimodal optoacoustic and multiphoton microscopy of human carotid atheroma," in Photoacoustics (2016).
- [27] Gasser, T.C., Ogden, R.W., and Holzapfel, G. a., "Hyperelastic modelling of arterial layers with distributed collagen fibre orientations.," Journal of the Royal Society, Interface / the Royal Society 3(6), 15–35 (2006).
- [28] Rekhter, M.D., "Collagen synthesis in atherosclerosis: too much and not enough," Cardiovascular Research 41, 376–384 (1999).
- [29] Pasterkamp, G., and Virmani, R., "The erythrocyte: a new player in atheromatous core formation.," Heart (British Cardiac Society) 88(2), 115–6 (2002).
- [30] Finn, A. V, and Jain, R.K., "Coronary Plaque Neovascularization and Hemorrhage," JACC Cardiovasc Imaging 3(1), 41–44 (2010).
- [31] Dima, A., and Ntziachristos, V., "Non-invasive carotid imaging using optoacoustic tomography," Optics Express 20(22), 25044 (2012).